Comparative Genomics of *Staphylococcus* Reveals Determinants of Speciation and Diversification of Antimicrobial Defense.

Rosanna Coates-Brown[1§], Josephine Moran[1], Pisut Pongchaikul[1¶], Alistair Darby[1] and Malcolm J. Horsburgh[1*]

[1]Institute of Integrative Biology, University of Liverpool, Liverpool, Merseyside, United Kingdom.

§ Present address: Genomic Diagnostic Laboratory, St Mary's Hospital, Oxford Road, Manchester, UK

¶Present address: Faculty of Medicine Ramathibodi Hospital, Mahidol University, 270 Rama IV Road, Ratchathewi, Bangkok, 10400, Thailand

* Corresponding author: Institute of Integrative Biology, University of Liverpool, Liverpool, L69 7ZB, United Kingdom.

Email: M.J.Horsburgh@liverpool.ac.uk

Tel: +44 1517954569

Fax +44 1517954410

Abstract

The bacterial genus *Staphylococcus* comprises diverse species with most being described as colonizers of human and animal skin. A relational analysis of features that discriminate its species and contribute to niche adaptation and survival remains to be fully described. In this study, an interspecies, whole-genome comparative analysis of 21 *Staphylococcus* species was performed based on their orthologues. Three well-defined multi-species groups were identified: group A (including *aureus*/*epidermidis*); group B (including *saprophyticus*/*xylosus*) and group C (including *pseudintermedius*/*delphini*). The machine learning algorithm Random Forest was applied to identify variable orthologues that drive formation of the *Staphylococcus* species groups A-C. Orthologues driving staphylococcal infrageneric diversity comprised regulatory, metabolic and antimicrobial resistance proteins. Notably, the BraSR (NsaRS) two-component system (TCS) and its associated BraDE transporters that regulate antimicrobial resistance distinguish group A *Staphylococcus* species from others in the genus that lack the BraSR TCS. Divergence of BraSR and GraSR antimicrobial peptide survival TCS and their associated transporters was observed across the staphylococci, likely reflecting niche specific evolution of these TCS/transporters and their specificities for AMPs. Experimental evolution, with selection for resistance to the lantibiotic nisin, revealed multiple routes to resistance and differences in the selection outcomes of the BraSR-positive species *S. hominis* and *S. aureus*. Selection supported a role for GraSR in nisin survival responses of the BraSR-negative group B species *S. saprophyticus*. Our study reveals diversification of antimicrobial-sensing TCS across the staphylococci and hints at differential relationships between GraSR and BraSR in those species positive for both TCS.

Importance

The genus *Staphylococcus* includes species that are commensals and opportunist pathogens of humans and animals. Identifying the features that discriminate species of staphylococci is relevant to understanding niche selection and the structure of their microbiomes. Moreover, the determinants that structure the community are relevant for strategies to modify the frequency of individual species associated with dysbiosis and disease. In this study, we identify orthologous proteins that discriminate genomes of staphylococci. In particular, species restriction of a major antimicrobial survival system, BraSR (NsaRS), to a group of staphylococci dominated by those that can colonize human skin. The diversity of antimicrobial sensing loci was revealed by comparative analysis

and experimental evolution with selection for nisin resistance identified the potential for variation in antimicrobial sensing in BraRS-encoding staphylococci. This study provides insights into staphylococcal species diversity.

Introduction

Staphylococcus species and genomics

The existence of taxonomically distinct species groups was first proposed for *Staphylococcus* based on differential DNA-DNA hybridization methods (1). These groups were supported by 16S rDNA sequence analysis of 38 taxa (2) and multilocus sequence data of around 60 species and subspecies (3).

A comparative analysis that utilized next generation genome sequencing data of staphylococci to probe phylogenetic relationships with 491 shared orthologues across 12 *Staphylococcus* species (4) proposed *S. pseudintermedius* then *S. carnosus* as basal lineages. Moreover, with ten species in their analysis being residents of human skin, the authors proposed that evolution selected for human adaptation after branching from *S. carnosus*. The relationships between the strains generated from shared orthologues were maintained using total gene content (4). However, in contrast to the conclusions of 16S rDNA and multilocus data (2,3) their analysis revealed discrete clustering of *Staphylococcus* species. No distinct clustering of *S. hominis* with *S. haemolyticus* was observed and *S. saprophyticus* was assigned to the *S. epidermidis* group of species (4). Currently, there is a knowledge gap in *Staphylococcus* species comparisons with a need to determine if this clustering of staphylococcal species is supported using whole genome data. Our findings here begin to close this gap.

Two component systems

Prokaryotes are receptive to environmental stimuli through diverse sensory and transducing two component systems (TCS). These TCS archetypically comprise a sensor histidine kinase (HK) that spans the cell membrane to interact with the external environment. Stimulus perception causes conditional autophosphorylation that is relayed to an interacting response regulator (RR) to enable DNA-binding directed transcription modulation (5).

While TCS are widespread and diverse across prokaryotes, the intramembrane-sensing histidine kinases (IM-HK) are specific to the Firmicutes. This family of small HKs has a

short, 25 amino acid linker region between each 400 amino acid transmembrane helix. *S. aureus* GraSR uses a IM-HK to regulate a global network responsible for resistance to antimicrobial peptides (AMPs). GraSR modulates the expression of DltABCD and MprF that in concert alter the *S. aureus* surface charge to evade electrostatic interaction-mediated targeting of cationic AMPs (6).

An orthologous TCS to GraSR described in *S. aureus* was concurrently designated BraSR and NsaSR by two different groups (7,8). Serial passage in sub-MIC concentrations of the lantibiotic nisin was shown to select increased nisin MIC due to a SNP in *nsaS* gene encoding sensor histidine kinase of NsaRS (nisin susceptibility-associated sensor regulator) (8). The TCS was separately designated BraSR (bacitracin resistance-associated sensor regulator) from the reduced MIC of bacitracin and nisin determined for the TCS gene mutant (7). BraR binding sites were revealed upstream of the ABC transporter genes *braDE* and *vraDE* that were not transcribed in the mutant but induced in the presence of bacitracin. The transporter BraDE contributes to the detection of nisin and bacitracin and subsequent signal transduction via BraSR, whereas VraDE is more directly involved in detoxification by efflux (7). Transcription of *braSR* is increased following exposure to multiple antibiotics, including ampicillin, phosphomycin and nisin. Inactivation of *braS* (*nsaS*) revealed differential transcription of 245 genes (9), revealing the TCS might report cell envelope stress to directly regulate biofilm formation, cellular transport and responses to anoxia.

In this study, a comparative genome analysis of 21 *Staphylococcus* species was performed based upon their orthologous gene content. Species groups were revealed and then interrogated using the Random Forest algorithm to identify group-contributing genes. The operon encoding the BraSR TCS was found to differentiate the *S. aureus/S. epidermidis* species group from other species groups. Experimental evolution of representative *braSR*-positive and -negative species with nisin selection identified differential selection of BraSR and GraSR to produce resistance to this AMP.

Results and Discussion

Analysis of orthologous gene content across the staphylococci

The orthologous gene content of 21 sequenced staphylococcal species' genomes was determined using OrthoMCL to group orthologous genes (homologues separated by speciation) into clusters across the different species. The number of shared orthologous clusters between the different species' genomes was then represented as a heatmap (Figure 1). The output from this analysis revealed the assembly of three major groups of species, each with high numbers of shared orthologous clusters. An associated cladogram supported three groups (groups A, B and C) when defined as containing three or more species (Figure 1). This supported previous reported groupings from 16S rDNA and multilocus analyses (2,3). Presented here, three species pairs showed a high degree of shared orthologous clusters of genes and branched together in the cladogram: *S. aureus*/*S. simiae*, *S. simulans*/*S. carnosus*, and *S. lentus*/*S. vitulinus*.

The largest and least well-defined, species group comprises *S. epidermidis*, *S. capitis*, *S. warneri*, *S. haemolyticus*, *S. hominis*, *S. lugdunensis*, *S. pettenkoferi*, *S. aureus* and *S. simiae* (Figure 1). Designated group A, it is dominated by species that colonize human skin (20,21). The likelihood of a strain-dependent effect structuring group A was investigated by substituting *S. epidermidis*, *S. hominis* and *S. aureus* strains (Supplementary File S1). Substituting these individual species with alternative strains and repeating the OrthoMCL analysis did not alter species groupings. Groups B and C were similarly unaffected by switching strains of *S. saprophyticus* and *S. pseudintermedius*, respectively. Within group A, *S. aureus* and *S. simiae* are most related in the cladogram; these species were proposed as members of the *S. aureus* group of staphylococci from gene content (2).

The smaller species group B comprises *S. equorum*, *S. arlettae*, *S. cohnii*, *S. saprophyticus* and *S. xylosus* (Figure 1). Though not universal, a frequent lifestyle identified in the group B species is human or animal host colonization; several species are associated with meat products and novobiocin resistance (22, 23) with commonalities in their cell wall composition (24).

Species group C comprises *S. pseudintermedius*, *S. delphini* and *S. intermedius* and this collective was previously designated the *S. intermedius* group (SIG); the species cause opportunistic infection of companion animals and equids (22). Emerging antibiotic

resistance in the SIG species group is a clinical veterinary concern (25) and their routine speciation is complicated by their high degree of 16S rRNA locus sequence identity (26).

Genetic determinants directing the formation of species group A were tested in R using machine learning with the Random Forests algorithm for classification (27). This algorithm was used to identify variables, in this case OrthoMCL clusters, that contributed to formation of the groups, based on a forest of trees generated from these variables. OrthoMCL clusters representing each variable were determined and mapped back to respective genomes for each cluster and the PROKKA annotation of each protein coding sequence was verified using BLAST. Contributing variables were assigned for group A, based on the strain set described in Table 1, where permutations were used to verify the existence and reproducibility of species groups (Supplementary File S1).

Clusters driving formation of group A species

The presence of 15 and absence of 9 OrthoMCL clusters collectively contribute to defining group A, with differing levels of support (Mean Decrease in Accuracy [MDA] values) (Table 2 & Supplementary File S2). Lower MDA values correspond with the incomplete presence of orthologous clusters within all species in a group. Several strongly supported orthologues contribute to group A (Table 2), notably the presence of four that are sequentially encoded in the genome as an operon (epi_02134 - epi_02137; MDA 3.2, 3.0, 2.6, 2.2, respectively). The latter cluster pair epi_02136/epi_02137 was annotated by PROKKA as a TCS sensor/regulator (Table 2 & Supplementary File S2) and shares ~100% similarity with BraSR (SA2417/SA2418 of *S. aureus* N315), a TCS associated with resistance to AMPs nisin and bacitracin (7). The adjacent clusters encoded in the same operon (epi_02134, epi_02135) comprise the BraD/BraE ABC transporter subunits with 98% and 99% similarity with SA2415/ SA2416 of *S. aureus* N315, respectively (7). We demonstrate as a key finding of our analysis that the genomes of group A *Staphylococcus* species uniquely contain BraSR and BraDE.

The presence of orthologue epi_00542 (MDA 2.2; Table 2 & Supplementary file S2) contributes to species group A, with support that the protein functions as a putative cell wall hydrolase from the Nlp-P60 family hydrolase domain that is associated with hydrolysis of peptidoglycan. Also, contributing to defining group A are the absences of two orthologue clusters (sap_00398; MDA 3.3 and sap_00399; MDA 1.4; Table 2 & S2) that are annotated as multidrug ABC transporters. A range of cytotoxic molecules are

mobilized across the cell membrane by multidrug ABC transporters where certain families of these can also act as sensors (5, 28). Across staphylococcal groups, differential repertoires of ABC transporters associated with antimicrobial survival are consistent with the importance of community competition in species evolution.

Sequence variation of the NADP-dependent succinate semialdehyde dehydrogenase (SSADH) between group A staphylococci versus groups B and C was identified by the association of cluster sap_00201 (MDA 2.9, Table 2 & Supplementary File S2) with group A species; this variation might be allied to differences in glutamate metabolism across the genus. Glutamate is involved in multiple metabolic processes and bacterial glutamate dehydrogenase catabolizes glutamate, which contributes to acid tolerance. NADP-SSADH catalyzes catabolism of γ-aminobutyrate, a product of glutamate dehydrogenase activity (29); this pathway is oxidative stress sensitive owing to the catalytic cysteine residue of SSADH.

Clusters driving formation of group B and C species

The size of species input groups B and C (Figure 1) used here limits use of the random forest algorithm and a broader species comparison of staphylococci could be considered in future. Consequently, a similar species-defined analysis of groups B and C was not pursued beyond a cursory view. Of note, however, a unique discriminating orthologue of group B was identified that supports broader species analyses. This orthologue is annotated as squalene synthase (SQS), a farnesyl diphosphate:farnesyl transferase (xylosus_00489; Supplementary File S3). SQS catalyzes an alternative pathway for the biosynthesis of carotenoid pigments (30). In *S. aureus*, biosynthesis of the carotenoid staphyloxanthin is catalyzed by the dehydrosqualene synthase CrtM, which converts farnesyl diphosphate (FPP) to dehydrosqualene (31). A recent study has determined that combining the activities of SQS and dehydrosqualene desaturase (CrtN) was sufficient to synthesize the carotenoid pigment staphyloxanthin by combining *E. coli* and *S. aureus* enzymes, respectively (31). Experimentation is required to determine catalytic specificity of the putative *Staphylococcus* group B-associated SQS. The *S. saprophyticus* protein has 13.24% similarity with *S. aureus* CrtM and 28% similarity with *Methylomonas* SQS. In support of differential substrate inputs, group B staphylococci such as *S. xylosus* and *S. arlettae* also encode CrtM in addition to CrtPQN necessary for staphyloxanthin biosynthesis.

Diversity of cationic AMP survival loci across the staphylococci

The described comparative genomic analysis revealed that while BraSR TCS is restricted to group A species of staphylococci, the GraSR TCS is distributed across all species groups. Supporting predictions from the Random Forest analysis, low sequence identity of BraR/BraS with GraR/GraS was confirmed. BraR mean sequence identity with GraR of group A (44%) and group B/C species (40%) was greater than that of BraS compared with GraS of group A and groups B/C (mean ~30% and ~26%, respectively) (Table 3).

High mean sequence identity (84-98%) of GraR regulator protein occurs within each of the three species groups (Table 3) with divergence of GraR between species groups identified by lower mean sequence identity (67%). GraS sensor histidine kinase was less conserved within species groups A (mean 69%) and B (mean 66%), compared with GraS of species group C that shared greatest mean sequence identity (88%), albeit that group C defined here is a small, related species set. Both BraS and GraS sensor proteins have lower sequence conservation across staphylococci than BraR and GraR (Table 3). The reduced divergence of these response regulators might reflect their relative isolation from selection by the external environment and differential stimuli.

Responses to cationic AMPs in the staphylococci are complex (32) and ligand specificity could account for species divergence of GraSR and BraSR TCS. This evolutionary outcome could be explained with strong selection pressure driven by ubiquity and diversity of cAMPs in staphylococcal niches. One intrigue in our analysis is the absence of GraSR and presence of only BraSR TCS in the group A species, *S. pettenkoferi*, with the sole related sensor protein having a mean sequence identity of 27% with group A GraS but 58% with group A BraS. *S. pettenkoferi* BraR has a mean sequence identity of 47% with GraR and 73% with BraR from group A. These values support the *S. pettenkoferi* TCS is a BraSR orthologue and its singular association raises questions about the evolution of BraSR in group A staphylococci. Gene duplication of GraSR in a group A species, with subsequent sequence divergence over time to BraSR and spread throughout group A species by horizontal gene transfer, is tempting to suggest. *S. pettenkoferi* having BraSR but not GraSR presents a challenge to this paralogue hypothesis. We propose two possibilities; *S. pettenkoferi* may have suffered deletion of *graSR* following acquisition of *braSR*, or *S. pettenkoferi* never acquired *braSR*, but rather its TCS evolved from ancestral genes. Such a scenario would enable group A organisms to acquire *braSR* from *S. pettenkoferi* as an additional and sufficiently divergent TCS locus.

Regardless of the origins of both TCSs, the divergence between and within GraSR and BraSR likely reflect specificities for their ligands and selection driven by the niches to which the staphylococci are specialized.

GraSR and BraSR-associated ABC transporters

Both GraSR and BraSR, as members of the BceS-like IM-HK family of TCS, are activated by AMP ligand bound to an associated ABC transporter (33). Given the important function of these TCS, the conservation of their associated transporter protein sequences was compared across the staphylococci.

VraFG is the GraSR-associated ABC transporter (34) and in the genomes encoding VraFG (absent from group B species and *S. pettenkoferi*) there is a high degree of shared protein sequence conservation. VraF has a mean sequence identity of 68% across the staphylococci examined (Table 1), with greatest conservation within species groups (group A, 79% identity; group B, 85.3% identity; group C, 96.8% identity). Shared sequence identity among the VraG proteins was 47.5%, with 88%, 65.2% and 61.9% identity within groups A, B and C, respectively. The BraDE ABC transporter associated with BraSR was identified in group A species and, similar to VraFG, revealed greater identity (68.4%) across BraD sequences compared with BraE (38.9%) protein sequences. Divergence within BraSR and GraSR-associated transporters has likely arisen from concurrent evolution of the ABC transporter specificities for AMPs.

Experimental evolution of nisin resistance in *S. aureus*, *S. hominis* and *S. saprophyticus*.

Previous studies demonstrated that selection by experimental evolution identified mutations conferring antimicrobial resistance in overarching regulators, notably SNPs in *braS* revealed roles for BraSR in nisin sensing and survival (7). Following our identified species restriction of BraSR to group A staphylococci, we adopted an experimental evolution strategy to interrogate the contributions of GraSR and BraSR TCS under selection for nisin resistance.

Strains of group A species, *S. aureus* and *S. hominis* plus group B *S. saprophyticus* were each serially passaged in triplicate cultures with increasing concentrations of nisin using a microtiter plate method, with an equivalent sodium citrate buffer control passaged in

parallel. Stepwise increases in nisin MIC were observed for all strains tested with no obvious pattern in the rate of resistance acquisition between the species. After selection, both *S. aureus* 171 and *S. aureus* SH1000 strains exhibited ~100-fold increases in nisin MIC, a greater fold increase in resistance than that observed by Blake *et al* (7), which may be due to experimental design differences. Selection of both *S. hominis* strains increased nisin MIC ~25-fold, and *S. saprophyticus* strains CCM_883 and CCM_349 showed 80-fold and 5-fold increases, respectively. Multiple clones of *S. aureus* 171, *S. hominis* J31 and *S. saprophyticus* CCM883 were genome sequenced to identify sequence variants that potentially contributed to increased nisin MIC. T0 genomes were assembled and annotated, then reads from three pools (each comprising 5 independent clones) and one individual clone of each experimentally evolved species were aligned to their respective assembled genomes to identify sequence variants (SNPs, insertions/deletions) specific to nisin selection (Tables 4-6).

Nisin-selected SNPs in staphylococci

Experimental evolution of *S. saprophyticus* identified a SNP in *graS* (GraS: $A_{160}S$; table 4) that was present in two clone pools, and SNP *graS* $G_{209}C$ in a third pool. A single clone sequenced from the latter pool identified only one SNP in *graS* (GraS: $G_{209}C$) and an upstream variant associated with *ptsG* (table 4). These data provide support for GraSR contributing to nisin resistance in *S. saprophyticus* given the absence of the BraSR TCS in this group B *Staphylococcus* species. Aside from TCS, other regulators may contribute to the nisin response in *S. saprophyticus* as evidenced by an identical SNP identified in two separate nisin resistance selections (pools 2 and 3) corresponding to a $T_{62}I$ change in an uncharacterized MarR transcriptional repressor.

In both *S. aureus* and *S. hominis* there are multiple pathways to high-level nisin resistance. Each species revealed SNPs in TCS systems, but these differed across the parallel selection experiments (Table 4-6). In *S. aureus*, a non-synonymous SNP in *braS* (BraS: $T_{175}I$) was present in 100% of reads from one sequenced pool, differing from previous work that identified a discrete *braS* SNP (BraS: $A_{208}E$) (7). Evidence for a second TCS contributing to nisin resistance arose from a *walK* non-synonymous SNP (WalK: $H_{364}R$) within the diverse and flexible signal sensing PAS domain of WalK in *S. aureus* (35). WalKR is essential and functions to maintain cell wall metabolism (36) and SNPs in this TCS contribute to vancomycin and daptomycin resistance due to cell wall-thickening (37). Should this cell wall phenotype be associated with the $H_{364}R$ WalK

variant it could similarly limit nisin interaction with its lipid II target to abrogate pore formation. A large overlap was reported between the WalKR and GraSR regulatory networks in *S. aureus* (6).

In *S. hominis*, a *graS* SNP (GraS: $S_{120}L$) was present in 2 clones of sequence pool 2 and no SNPs or other sequence variants were identified in *braSR* (Table 4-6). *S. hominis* has both *braSR* and *graSR* loci and therefore it is intriguing nisin resistance selection resulted in SNPs in a different TCS to *S. aureus* despite encoding both, potentially reflecting differences in their contribution across group A staphylococci. A further transcriptional regulator might contribute to nisin resistance in both *S. aureus* and *S. hominis*, where the uncharacterized *yhcF* revealed SNPs producing $G_{73}R$ and $N_{47}*$, respectively; the presence of SNPs in *yhcF* of both species supports a role for this regulator. The YhcF transcriptional regulator proteins of *S. aureus* and *S. hominis* have 75% similarity and their cognate genes are adjacent to an ABC transporter locus with potential specificity for GlcNAc, which might catalyze recycling of cell wall substrates from nisin damage. The role of this operon is currently being investigated.

In summary, we have identified differential encoding and diversity of antimicrobial resistance regulators and their associated transporters across the staphylococci. Our previous studies of the nasal microbiome correlated cumulative antimicrobial production with community structure, limitation of invasion and *S. aureus* exclusion (38, 39, 40). Further dissection of antimicrobial sensing and discrimination via the TCS systems BraSR and GraSR combined with analysis of their associated transport specificities will provide information that can be layered with niche-relevant antimicrobial activities from competing species. Such analyses are now emerging and will provide a more holistic determination of *Staphylococcus* ecology.

Methods

Staphylococcus orthologous gene content

Representative genomes of 21 different *Staphylococcus* species available at the time of analysis (Table 1) were either sequenced (see later section) or retrieved from the NCBI FTP repository (ftp://ftp.ncbi.nlm.nih.gov/). Complete genomes were used where possible. Draft genomes available as NCBI scaffolds were reordered against an appropriate reference using a bespoke perl script. Genomes were annotated using PROKKA (version 1.5.2) (41) to ensure consistent gene calling and annotation.

OrthoMCL (version 1.4) was used to cluster orthologous proteins (42), with input parameters, e-value cut-off: 1e-5, percentage identity cut-off: 30, percentage match cut off: 20. A bespoke python script was used to create a table describing the presence or absence of each OrthoMCL cluster within every genome. These data were converted to a matrix for analysis in the statistical package R and a heatmap was generated from the matrix. To control for gross strain-specific effects on the heat map (and thus OrthoMCL clusters), this step was repeated by substituting with alternative strains (Table S1) and all permutations were analyzed in subsequent steps of the analysis.

Drivers of OrthoMCL group formation

The R library, Random Forest (version 4.6-7) (43) was used to investigate the genetic inputs directing classification of the species into their OrthoMCL groups. A presence/absence table of each of the orthologous groups obtained from the USA300 permutation of the OrthoMCL analysis was generated using a bespoke python script and used as the input data for the Random Forest algorithm.

The data was split into a test and training data set with both sets including equal proportions of group A species. The optimum value for mtry was found to be 66 using the tuneRF function (ntree=1001, stepFactor=1.5, improve=0.001). These mtry and ntree parameters resulted in a model with an out of bag error rate of 9.09%.

Data output was summarized using the variable importance plot function and the numeric mean decrease in accuracy (MDA) resulting from the permutation of each variable was obtained through the importance function; these data were used as the measure of the importance of each variable. The maximum MDA in this analysis was 3.3. Clusters were mapped back to the genome and the annotation of protein sequence for a species representative of each cluster was retrieved. Protein sequences of clusters identified as important were retrieved and their annotations curated and verified against published annotations. In addition, outputs were generated by substituting strains of species in the analysis to compare conservation of identified clusters between the variable importance plots. Sequences of protein clusters from the single species representative in Table 2 and identified by Random Forest output are listed in Supplementary Files S2-3. Protein sequences were retrieved from their respective genomes and alignments were performed using ClustalW2 (version 2.1).

Minimum inhibitory concentration assay

Nisin (Sigma-Aldrich Company Ltd, UK) was prepared as a 20 mg mL^{-1} solution in 10 mM sodium citrate (Sigma-Aldrich Company Ltd, UK) at pH 3 and stored at 4 °C. MIC assay used microtiter plates with doubling dilutions of nisin in BHI (Thermo Scientific) inoculated 1 in 2 with 100 µL bacterial suspension adjusted to OD_{600} 0.2 ± 0.005. The lowest concentration with an optical density ≤ to that of the initial optical density was taken as the minimum inhibitory concentration (MIC).

Selection for nisin resistance

Experimental evolution was performed by serial passage in broth containing doubling dilutions of nisin in triplicate wells of a microtiter plate. For selection of *S. aureus* and *S. saprophyticus*, the maximal assay concentration of nisin was 5 mg mL^{-1} and for *S. hominis* 50 µg mL^{-1}. Control selection experiments with equivalent sodium citrate concentrations were performed in parallel. Experiments were initiated with inoculation of bacteria to OD_{600} =0.2 for the first passage and plates were incubated static at 37 °C. Bacteria growing at the highest concentration of nisin after 24-48 h were passaged forward to the next plate; subsequent passages were inoculated with a 1:1000 dilution of culture. Serial passage was continued until growth occurred at the maximal nisin concentration (for strains *S. saprophyticus* =10 mg ml^{-1}, *S. aureus* =10 mg ml^{-1} and *S. hominis* =250 µg ml^{-1}) or for a period of 12 days. All passaged cultures were collected and stored at -80ºC in 20% (v/v) glycerol (Fisher Scientific) after each passage and the T_0 time point served as comparator strain.

Colonies were randomly selected for sequencing after plating from independent biological replicate cultures that had reached an equivalent maximum level of nisin resistance. Clones from each repeat were selected and cultured in 10 mL of BHI at 37 °C with shaking at 200 rpm overnight. Increased MICs were confirmed by using the MIC assay described above at the highest nisin concentrations. Selection was performed for a corresponding citrate control time point for each of the three species.

DNA extraction, library preparation and sequencing

Cells were harvested from overnight culture and lysed in buffer containing 12.5 µg ml^{-1} lysostaphin (Sigma-Aldrich) and 10 U mutanolysin (Sigma-Aldrich). DNA was purified using a DNeasy Blood and Tissue Kit (Qiagen). DNA (30 ng) from each of five selected clones was pooled to make Illumina Truseq DNA libraries with an insert size of 350 bp. In addition to three separate clone pools, a single clone was selected for sequencing from the

clones used to constitute the pools. Single clones were selected on the basis of the highest DNA quality. The single clones and the T_0 isolates were also sequenced using Illumina Truseq nano DNA libraries with 350 bp inserts.

Identification of SNPs and INDELS

T_0 comparator strains were assembled using VelvetOptimiser (version 2.2.5; Victoria Bioinformatics Consortium) with Kmer sizes from 19 to 99 and Velvet version 1.2.06 (45). Annotation was carried out using PROKKA version 1.5.2 (Seemann 2014). The PacBio assembly of *S. hominis* strain J31 (Accession FBVO01000000) (46) was used as the comparator assembly for this strain. Good quality filtered reads from experimentally evolved pools and single clones were aligned to respective comparator strains using the BWA (version 0.5.9-r16) (47) packages aln and sampe, and also using BWA (version 0.7.5a-r405) mem package. SAM files were converted to bcf (binary variant call) files with samtools for SNP calling using the mpileup package. The bcf output file from mpileup was then converted to vcf (variant call format) files and quality filtered. For SNPs, only this quality filtered vcf file from the pooled clones, along with mpileup output without base data, were used to further filter the SNPs to include only those present in 33.33% of reads, which equates to the SNP being present in more than one clone. To reduce falsely called SNPs, SNPs not called from both alignments (from either BWA aln and sampe or BWA mem) were removed from the data set, as recommended by (48). SNPs called in the control data and evolved isolates were filtered from the data.

Data accession

Genomes resulting from this work can be retrieved from the ENA database at EMBL-EBI (https://www.ebi.ac.uk/ena/data/view) under the bioproject accession PRJEB22856, including data from experimental evolution of *S. aureus* 171; Parental *S. aureus* 171 data accession: LT963437. Individual genome assembly accessions used in Figure 1 are listed in Table 1 and Supplementary File S1.

Conflicts of interest

RC-B was funded by BBSRC training grant BB/J500768/1 awarded to MJH with support from Unilever Plc. JM was funded by BBSRC research grant BB/L023040/1 awarded to MJH with support from Unilever Plc. The funders were not involved in the study design, collection of samples, analysis of data, interpretation of data, the writing of this report or the decision to submit this report for publication.

Acknowledgements

We are grateful to Dr Miriam Korte-Berwanger, University of Bochum and Prof Ross Fitzgerald, University of Edinburgh for kindly providing *Staphylococcus* strains used in this study.

References

1. Kloos WE, Schleifer, K-H, Götz R. 1991. The genus *Staphylococcus*. p 1369-1420. *In* Balows A, Trooper HG, Dworkin M, Harder W, Schleifer K-H. (ed.). The prokaryotes: a handbook on the biology of bacteria: ecophysiology, isolation, identification, applications, 2nd ed, vol. 2. Edited by New York: Springer.

2. Takahashi T, Satoh I, Kikuchi N. 1999. Phylogenetic relationships of 38 taxa of the genus *Staphylococcus* based on 16S rRNA gene sequence analysis. Int J Syst Bacteriol 49:725–728.

3. Lamers RP, Muthukrishnan G, Castoe TA, Tafur S, Cole AM, Parkinson CL. 2012. Phylogenetic relationships among *Staphylococcus* species and refinement of cluster groups based on multilocus data. BMC Evol Biol 12:171.

4. Suzuki H, Lefébure T, Bitar PP, Stanhope MJ. 2012. Comparative genomic analysis of the genus *Staphylococcus* including *Staphylococcus aureus* and its newly described sister species *Staphylococcus simiae*. BMC Genomics 13:38.

5. Stock AM, Robinson VL, Goudreau PN. 2000. Two-component signal transduction. Ann Rev Biochem 69:183–215.

6. Falord M, Mäder U, Hiron A, Débarbouillé M, Msadek T. 2011. Investigation of the *Staphylococcus aureus* GraSR regulon reveals novel links to virulence, stress response and cell wall signal transduction pathways. PLoS ONE 6:e21323.

7. Hiron A, Falord M, Valle J, Débarbouillé M, Msadek T. 2011. Bacitracin and nisin resistance in *Staphylococcus aureus*: a novel pathway involving the BraS/BraR two-component system (SA2417/SA2418) and both the BraD/BraE and VraD/VraE ABC transporters. Mol Microbiol 81:602–622.

8. Blake KL, Randall CP, O'Neill AJ. 2011. *In vitro* studies indicate a high resistance potential for the lantibiotic nisin in *Staphylococcus aureus* and define a genetic basis for nisin resistance. Antimicrob Agents Chemother 55:2362–2368.

9. Kolar SL, Nagarajan V, Oszmiana A, Rivera FE, Miller HK, Davenport JE, Riordan JT, Potempa J, Barber DS, Koziel J, Elasri MO, Shaw LN. 2011. NsaRS is a cell-envelope-stress-sensing two-component system of *Staphylococcus aureus*. Microbiology 157:2206–2219.

10. Dinakaran V, Shankar M, Jayashree S, Rathinavel A, Gunasekaran P, Rajendhran J. 2012. Genome sequence of *Staphylococcus arlettae* strain CVD059, isolated from the blood of a cardiovascular disease patient. J Bacteriol. 194:6615-6616.

518 11. Baba T, Bae T, Schneewind O, Takeuchi F, Hiramatsu K. 2008. Genome sequence of
519 *Staphylococcus aureus* strain Newman and comparative analysis of staphylococcal
520 genomes: polymorphism and evolution of two major pathogenicity islands. J Bacteriol
521 190:300-310.
522 12. Rosenstein R, Nerz C, Biswas L, et al. 2009. Genome analysis of the meat starter
523 culture bacterium *Staphylococcus carnosus* TM300. Appl Environ Microbiol 75:811-822.
524 13. Zhang YQ, Ren SX, Li HL, Wang YX, Fu G, Yang J, Qin ZQ, Miao YG, Wang WY,
525 Chen RS, Shen Y, Chen Z, Yuan ZH, Zhao GP, Qu D, Danchin A, Wen YM. 2003.
526 Genome-based analysis of virulence genes in a non-biofilm-forming *Staphylococcus*
527 *epidermidis* strain (ATCC 12228). Mol Microbiol 49:1577-93.
528 14. Nam Y-D, Chung W-H, Seo M-J, Lim S-I, Yi S-H. 2012.Genome sequence of
529 *Staphylococcus lentus* F1142, a strain isolated from Korean soybean paste. J Bacteriol
530 194:5987.
531 15. Tse H, Tsoi HW, Leung SP, Lau SKP, Woo PCY, Yuen KY. 2010. Complete genome
532 sequence of *Staphylococcus lugdunensis* Strain HKU09-01. J Bacteriol 192:1471-1472.
533 16. Tse H, Tsoi HW, Leung SP, Urquhart IJ, Lau SKP, Woo PCY, Yuen KY. 2011.
534 Complete genome sequence of the veterinary pathogen *Staphylococcus pseudintermedius*
535 strain HKU10-03, isolated in a case of canine pyoderma. J Bacteriol 193:1783-1784.
536 17. Kuroda M, Yamashita A, Hirakawa H, et al. 2005. Whole genome sequence of
537 *Staphylococcus saprophyticus* reveals the pathogenesis of uncomplicated urinary tract
538 infection. PNAS 102:13272-13277.
539 18. Nam Y-D, Chung W-H, Seo M-J, Lim S-I. 2012. Draft genome sequence of
540 *Staphylococcus vitulinus* F1028, a strain isolated from a block of fermented soybean. J
541 Bacteriol 194:5961-5962.
542 19. Cheng VWT, Zhang G, Oyedotun KS, Ridgway D, Ellison MJ, Weiner JH. 2013.
543 Complete genome of the solvent-tolerant *Staphylococcus warneri* strain SG1. Genome
544 Announce 1:e00038-13.
545 20. Schleifer K-H, Bell JA. 2015. *Staphylococcus*. p 1–43. *In* Bergey's Manual of
546 Systematics of Archaea and Bacteria. John Wiley & Sons.
547 21. Kloos WE. 1980. Natural populations of the genus *Staphylococcus*. Ann Rev
548 Microbiol 34:559–592.
549 22. Devriese LA, Schleifer KH, Adegoke GO. 1985. Identification of coagulase-negative
550 staphylococci from farm animals. J Appl Bacteriol 58: 45–55.
551 23. Bannerman TL, Wadiak DL, Kloos WE. 1991. Susceptibility of *Staphylococcus*
552 species and subspecies to teicoplanin. Antimicrob Agents Chemother 35:1919–1922.

553 24. Schleifer KH, Kilpper-Bälz R, Devriese LA. 1984. *Staphylococcus arlettae* sp. nov.,
554 *S. equorum* sp. nov. and *S. kloosii* sp. nov.: three new coagulase-negative, novobiocin-
555 resistant species from animals. Syst Appl Microbiol 5:501–509.
556 25. Stull JW, Slavić D, Rousseau J, Weese JS. 2014. *Staphylococcus delphini* and
557 methicillin-resistant *S. pseudintermedius* in horses, Canada. Emerg Infect Dis 20:485–
558 487.
559 26. Slettemeås JS, Mikalsen J, Sunde M. 2010. Further diversity of the *Staphylococcus*
560 *intermedius* group and heterogeneity in the MboI restriction site used for *Staphylococcus*
561 *pseudintermedius* species identification. J Vet Diagn 22:756–759.
562 27. Breiman L. 2001. Random forests. Machine Learning 45:5-32.
563 28. Rietkötter E, Hoyer D, Mascher T. 2008. Bacitracin sensing in *Bacillus subtilis*. Mol
564 Microbiol 68:768–785.
565 29. Feehily C. Karatzas KAG. 2013. Role of glutamate metabolism in bacterial responses
566 towards acid and other stresses. J Appl Bacteriol 114:11–24.
567 30. Tao L, Schenzle A, Odom JM, Cheng Q. 2005. Novel carotenoid oxidase involved in
568 biosynthesis of 4,4'-diapolycopene dialdehyde. Appl Environ Microbiol 71:3294–3301.
569 31. Furubayashi M, Li L, Katabami A, Saito K, Umeno D. 2014. Construction of
570 carotenoid biosynthetic pathways using squalene synthase. FEBS Lett 588:436–442.
571 32. Peschel A, Collins LV. 2001. Staphylococcal resistance to antimicrobial peptides of
572 mammalian and bacterial origin. Peptides. 22:1651-9.
573 33. Mascher T. 2014. Bacterial (intramembrane-sensing) histidine kinases: signal transfer
574 rather than stimulus perception. Trends Microbiol 22:559–565.
575 34. Meehl M, Herbert S, Götz F, Cheung A. 2007. Interaction of the GraRS two-
576 component system with the VraFG ABC transporter to support vancomycin-intermediate
577 resistance in *Staphylococcus aureus*. Antimicrob Agent Chemother 51:2679–2689.
578 35. Hefti MH, Françoijs KJ, de Vries SC, Dixon R, Vervoort J. 2004. The PAS fold. A
579 redefinition of the PAS domain based upon structural prediction. Eur J Biochem
580 271:1198–1208.
581 36. Delaune A. Dubrac S, Blanchet C, Poupel O, Mäder U, Hiron A, Leduc A, Fitting C,
582 Nicolas P, Cavaillon JM, Adib-Conquy M, Msadek T. 2012. The WalKR system controls
583 major staphylococcal virulence genes and is involved in triggering the host inflammatory
584 response. Infect Immun 80:3438–3453.
585 37. Howden BP, McEvoy CR, Allen DL, Chua K, Gao W, Harrison PF, Bell J, Coombs
586 G, Bennett-Wood V, Porter JL, Robins-Browne R, Davies JK, Seemann T, Stinear TP.
587 2011. Evolution of multidrug resistance during *Staphylococcus aureus* infection involves

588 mutation of the essential two component regulator WalKR. PLoS Pathog 7:e1002359.
589 38. Libberton B, Coates RE, Brockhurst MA, Horsburgh MJ. 2014. Evidence that
590 intraspecific trait variation among nasal bacteria shapes the distribution of
591 *Staphylococcus aureus*. Infect Immun 82:3811-3815.
592 39. Libberton B, Horsburgh MJ, Brockhurst MA. 2015. The effects of spatial structure,
593 frequency dependence and resistance evolution on the dynamics of toxin-mediated
594 microbial invasions. Evol Appl 8:738-750.
595 40. Coates R, Moran J, Horsburgh, MJ. 2014. Staphylococci: colonizers and pathogens of
596 human skin. Future Microbiol 9:75-91.
597 41. Seemann T. 2014. Prokka: rapid prokaryotic genome annotation. Bioinformatics
598 30:2068-2069.
599 42. Li L, Stoeckert CJ Jr, Roos DS. 2003. OrthoMCL: identification of ortholog groups
600 for eukaryotic genomes. Genome Res 13:2178–2189.
601 43. Liaw A, Wiener M. 2003. Classification and regression by randomForest. R News
602 2:18-22.
603 44. Zerbino DR, Birney E. 2008. Velvet: algorithms for *de novo* short read assembly
604 using de Bruijn graphs. Genome Res 18:821–829.
605 45. Coates-Brown R, Horsburgh MJ. Whole-genome sequence of *Staphylococcus hominis*
606 strain J31 isolated from healthy human skin. 2017. Genome Announc 5:e01548-16.
607 46. Li H, Durbin R. 2009. Fast and accurate short read alignment with Burrows-Wheeler
608 transform. Bioinformatics 25:1754–1760.
609 47. Li H. 2014. Towards better understanding of artifacts in variant calling from high-
610 coverage samples. Bioinformatics 30:2843-2851.
611
612
613
614
615

Figure Legends

Table 1. *Staphylococcus* species and strains included in OrthoMCL analysis. Genomes were sequenced for this study, as indicated, or retrieved from NCBI for analysis; genome integrity is indicated.

Figure 1. Heat map representation of shared orthologous proteins across *Staphylococcus* species. Presence is indicated using a color scale from red (highest number of shared clusters of orthologous proteins) to white (lowest number). Major groups of species observed in the analysis are highlighted as groups A-C

Table 2. Proteins driving formation of species group A. PROKKA annotation was found by mapping clusters from the variable importance analysis to the *S. epidermidis* genome in the case of 'present' clusters and the *S. saprophyticus* genome for 'absent' clusters. The PROKKA locus tag is indicated in brackets. BLAST homology was determined from searches against the NCBI BLAST database. %MDA is representative for the cluster across the randomForest analyses, where higher values indicate increased support.

Table 3. Comparative sequence identity of the BraRS and GraRS TCS across species groups A-C. Mean identity values of BraR and BraS within species group A and values for BraR and BraS with GraR and GraS of species group A or B/C. Mean identity values of GraR and GraS within and between species groups A, B and C. Sequence identity was calculated from multiple sequence alignments of all protein sequences of species indicated in Table 1.

Table 4. Non-synonymous, homozygous SNPs from independent clone pools of staphylococci after nisin selection. Pools comprise 5 clones from each of three independent experiments. Nisin MICs of clones in each pool were confirmed to ensure they were similar.

Table 5. Non-synonymous, homozygous SNPs from single clones of *S. aureus, S. hominis* and *S. saprophyticus* after nisin selection. Pools comprise 5 clones from each of three independent experiments. Nisin MICs of clones in each pool were confirmed to ensure they were similar.

Table 6. INDELs from nisin selection pools and single clones of *S. aureus, S. hominis* and *S. saprophyticus*. Insertion/deletion sequence change effects: frameshift (fs); upstream variant (uv); downstream variant (dv); deletion (del); insertion (ins). INDELs marked § are predicted to have a major consequence by SnpEFF.

File S1. *Staphylococcus* species and strains used as substitutes in OrthoMCL analyses.

File S2. Species group A, present and absent cluster protein sequences. Sequences represent clusters listed in Table 2.

File S3. Species group B orthologue sequence. Sequence of putative squalene synthase cluster of *S. xylosus*.

656 **Table 1**

657

Species	Strain	Accession	Status (Reference)
S. arlettae	CVD059	ALWK01000000 (Uid175126)	Draft (10)
S. aureus	Newman	AP009351 (Uid58839)	Complete (11)
S. capitis	SK14	ACFR01000000 (Uid55415)	Draft
S. carnosus	TM300	NC012121 (Uid59401)	Complete (12)
S. cohnii	ATCC29974	LT963440	Draft (This study)
S. delphini	8086	CAIA00000000 (Uid199664)	Draft
S. epidermidis	ATCC_12228	NC005008 (Uid57861)	Complete (13)
S. equorum	Mu2	CAJL01000000 (Uid169178)	Draft
S. haemolyticus	K8	LT963441	Draft (This study)
S. hominis	J6	LT963442	Draft (This study)
S. intermedius	NCTC_11048	CAIB01000000 (Uid199665)	Draft
S. lentus	F1142	AJXO01000000 (Uid200144)	Draft (14)
S. pettenkoferi	VCU012	AGUA00000000 (Uid180074)	Draft
S. lugdunensis	HKU09	CP001837 (Uid46233)	Complete (15)
S. pseudintermedius	HKU10	Uid62125	Complete (16)
S. saprophyticus	ATCC_15305	AP008934 (Uid58411)	Complete (17)
S. simiae	CCM_7213	AEUN0000000 (Uid77893)	Draft (4)
S. simulans	ATCC 27848	LT963435	Draft (This study)
S. vitulinus	F1028	AJTR0000000 (Uid200114)	Draft (18)
S. warneri	SG1	CP003668 (Uid187059)	Complete (19)
S. xylosus	ATCC29971	LT963439	Draft (This study)

658

659

660

661

662

663

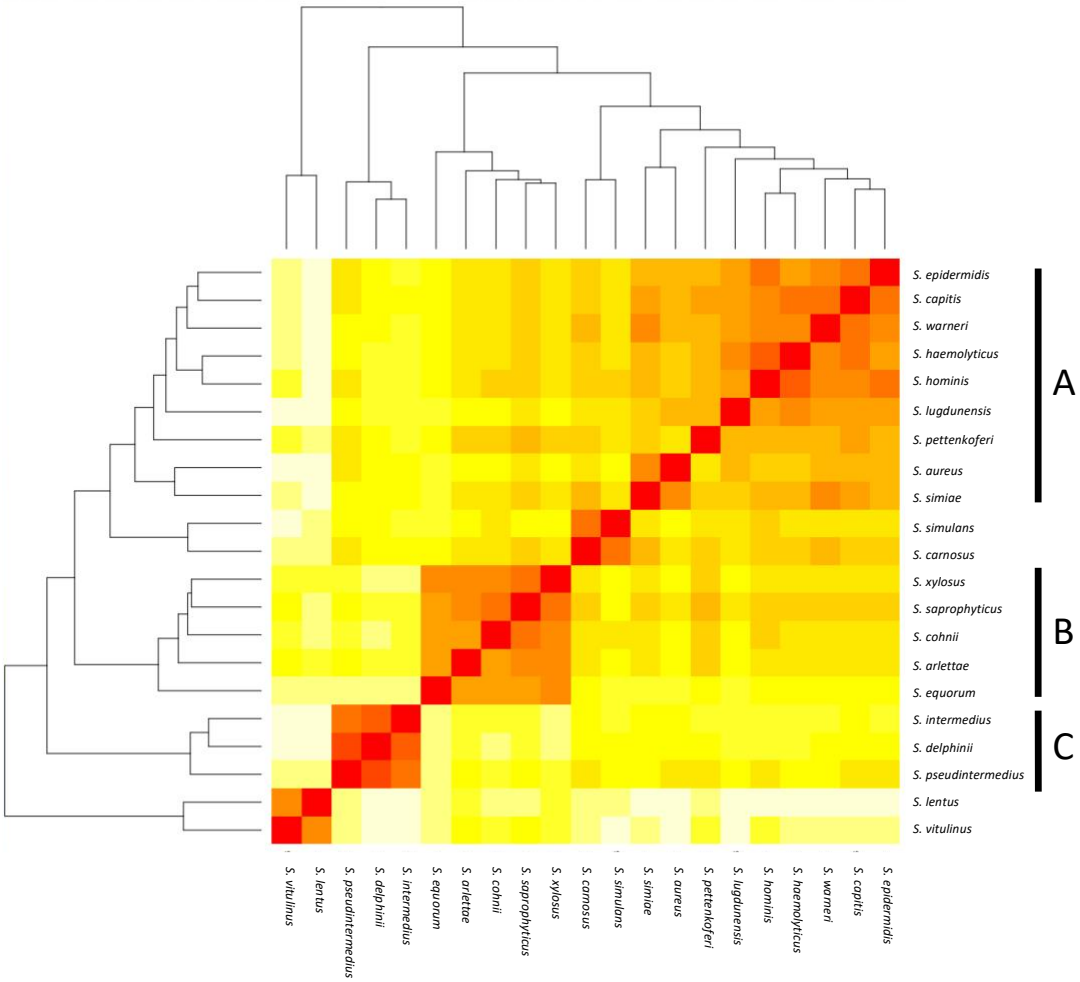

Figure 1

676

677

678

679 **Table 2**

Group A staphylococci		
PROKKA annotation	**BLAST homology**	**MDA**
Presence		
Putative cell wall associated hydrolase (epi_00542)	Hypothetical protein	2.2
Hypothetical protein (epi_02098)	Cell wall surface anchor protein	2.7
Hypothetical protein (epi_02108)	Hypothetical protein	1.9
FtsX like permease family protein (epi_02134)	ABC transporter permease	3.2
Macrolide export ATP binding/ permease protein MacB (epi_02135)	Bacteriocin ABC transporter ATP-binding protein	3.0
Sensor histidine kinase GraS (epi_02136)	TCS histidine kinase	2.6
Glycopeptide resistance associated protein R (epi_02137)	TCS transcriptional regulator	2.2
Absence		
Succinate semialdehyde dehydrogenase NADP+ (sap_00201)	Succinate-semialdehyde dehydrogenase	2.9
Putative membrane protein putative toxin regulator (sap_00203)	PTS sugar transporter subunit IIC	2.7
Putative multidrug resistance ABC transporter ATP binding/permease protein YheI (sap_00398)	Multidrug ABC transporter ATP-binding protein	3.3
Putative multidrug resistance ABC transporter ATP binding/permease protein YheH (sap_00399)	Multidrug ABC transporter ATP-binding protein	1.4
L-lactate utilization operon repressor (sap_00760)	Transcriptional regulator	2.7
Glutamate aspartate carrier protein (sap_01003)	Sodium:dicarboxylate symporter	2.7

680

681

682

683

684

685

686

687

688

Table 3

TCS protein	Mean identity within group A	Mean identity to groups B & C GraR or GraS	Mean identity to group A GraR or GraS
BraR	77.1	39.6	44.34
BraS	62.9	26.4	29.8

TCS protein	Mean identity within group A	Mean identity within group B	Mean Identity within group C	Mean Identity across groups
GraR	87.8	84	97.9	66.7
GraS	69.4	66	88.2	48.2

703 **Table 4**
704

Gene ID (Prokka)	Protein ID	Pool	Position	Base change	Amino acid change	Allele frequency
***S. aureus* 171**						
walK	WalK Sensor kinase	1	17119	A -> G	$H_{364}R$	1
gltB_1	Glutamate synthase	1	437361	A -> T	$Q_{797}L$	1
rpoB	DNA-directed RNA polymerase subunit beta	1	520176	C -> T	$H_{506}Y$	1
mraY	Phospho-N-acetylmuramoyl-pentapeptide transferase	1	1103071	G -> A	$V_{266}I$	1
yhcF	Transcriptional regulator	1	1998279	G -> A	$G_{73}R$	1
hypothetical	Membrane protein	2	615003	C -> T	Q_{57}*	0.35
rpoC	DNA-directed RNA polymerase subunit beta	3	523690	G -> T	$A_{448}S$	0.99
femB	FemB	3	1323450	G -> A	$R_{215}H$	0.63
phage terminase	Terminase	3	1491745	G -> C	$G_{240}A$	1
greA	GreA	3	1625376	A -> T	L_{76}*	0.37
braS	BraS sensor histidine kinase	3	2627088	C -> T	$T_{175}I$	1
***S. hominis* J31**						
rpoB	DNA-directed RNA polymerase subunit beta	1	41317	G -> T	$D_{1046}Y$	0.79
graS	GraS sensor histidine kinase	2	147503	C -> T	$S_{120}L$	0.42
ftsH	FtsH Zinc metalloprotease	2	2172470	C -> A	$D_{171}E$	1
gmk	Guanylate Kinase	3	552630	G -> A	$R_{135}H$	1
yhcF	Transcriptional regulator	3	1212777	C -> T	Q_{47}*	1
***S. saprophyticus* 883**						
graS	GraS sensor histidine kinase	1	2068987	G -> T	$G_{209}C$	1
codY	CodY regulator	2,3	1537681	C -> A	$L_{79}F$	1,1
pitA	Phosphate transporter	2,3	2066724	C -> T	$A_{195}V$	0.99,1
graS	GraS sensor histidine kinase	2,3	2069134	C -> A	$R_{160}S$	1,1
marR family	MarR regulator	2,3	2136907	C -> T	$T_{62}I$	1,1

705
706
707
708
709
710
711
712
713
714
715
716
717
718
719
720
721

722 **Table 5**
723

***S. aureus* strain 171 (single clone from pool 1)**				
Gene ID (Prokka)	**Protein ID**	**Position**	**Base change**	**Amino acid change**
walK	WalK Sensor histidine kinase	17119	A -> G	$H_{364}R$
gltB_1	Glutamate synthase	437361	A -> T	$Q_{797}L$
rpoB	DNA-directed RNA polymerase subunit beta	520176	C -> T	$H_{506}Y$
mraY	Phospho-N-acetylmuramoyl-pentapeptide transferase	1103071	G -> A	$V_{266}I$
msrR	Regulatory protein MsrR	1309845	G -> T	E_{181}*
yurK	Transcriptional regulator	1998279	G -> A	$G_{73}R$
***S. hominis* strain J31 (single clone from pool 2)**				
ftsH	Zinc metalloprotease FtsH	2172470	C -> A	$D_{171}E$
***S. saprophyticus* strain 883 (single clone from pool 1)**				
graS	GraS sensor histidine kinase	2068987	G -> T	$G_{209}C$

724
725
726
727
728
729
730
731
732
733
734
735
736
737
738
739
740
741
742
743
744
745
746
747
748
749
750

751
752 **Table 6**
753

Source	Gene ID (Prokka)	Protein ID	Location	Base change	Effect
***S. aureus* 171**					
Single, Pool 3	*lpl2_2*	Lipoprotein	403168	195_196 insGG	I66fs §
Single, Pool 1,3	*sdrE_1*	MSCRAMM family adhesin	554844	2672_2673 insC	K891fs §
Single			1990375	-1_-1 insCC	uv
Single, Pool 2,3			2052262	*1530_*1530 delTG	fs
Single, Pool 3	*deoC2*	Deoxyribose-phosphate aldolase 2	2126552	450_451 insAG	K151fs §
Single, Pool 1	hypothetical	Hypothetical protein	2471437	116_117 insT	E40fs
Single, Pool 3	*fnbA_2*	Fibronectin binding protein	2490720	1763_1764 delCG	S588fs §
Pool 1	hypothetical	Hypothetical protein	1556011	201 delT	S67fs §
Pool 2			1337112	-1_-1 insATG	
Pool 2,3	hypothetical	transposase	1337623	209_211 delAAG	E70del
Pool 2	hypothetical	transposase	1819467	1047_1048 insC	*350fs §
Pool 2	*leuA_2*		2052046	*1530 delC	dv
Pool 2	hypothetical	hypothetical	2471438	115_116 insATA	P39del, insHT
Pool 3	*lpl2_1*	hypothetical	402338	212_213 insCT	Q71fs §
Pool 3	*sdrD_1*	MSCRAMM family adhesin	550856	3237_3238 insC	M1080fs §
Pool 3	hypothetical		555082	-1_-1 insG	
Pool 3	hypothetical	LPXTG surface protein	2480756	216 delA	T72fs §
***S. hominis* J31**					
Single, Pool 2	*ftsH*	Zinc metalloprotease	2172279	325 delA	S109fs §
Pool 1	*relA*	GTP Pyrophosphokinase	951655	764 delA	Q255fs §
Pool 2	*ssaA2_2*	CHAP domain containing protein	1437614	575_578 delGTTA	G192fs §
***S. saprophyticus* 883**					
Single, Pool 1,2,3	*ptsG*	PTS alpha-glucoside transporter subunit IIBC	604054	-1_-1 insAA	uv